Effect of multiple debris flow countermeasures on flow characteristics and topographic changes through real-scale experiment

Woojae Jang[2], *Beom-Jun* Kim[1], *Shin-Kyu* Choi[3], *Tae-Hyuk* Kwon[2] and *Chan-Young* Yune[1*]

[1]Gangneung-Wonju National University, Department of Civil Engineering, 25457 Gangneung, South Korea
[2]Korea Advanced Institute of Science and Technology, Department of Civil and Environmental Engineering, 34141 Daejeon, South Korea
[3]Korea Electric Power Research Institute, 34056 Daejeon, South Korea

Abstract. In this study, to investigate the effect of multiple countermeasure on the flow characteristics of debris flows, a real-scale experiment was conducted in a natural gully by reproducing a debris flow with a installation of multiple countermeasures. In addition, the topographic changes before and after experiment by debris flow were investigated using UAV-LiDAR. Based on the experiment results, the effect of multiple countermeasures and the topographic changes against the gully erosion and deposition caused by debris flow were also analyzed. The installation of multiple countermeasures significantly decreased the frontal velocity of debris flow. Furthermore, the countermeasure induced the deposition of debris material on the back of the countermeasure.

1 Introduction

Debris flows can lead disastrous consequences to downstream infrastructure of societies because of its fast-moving characteristics along valleys [3, 4]. Structural countermeasures have been widely utilized to prevent debris flow hazards, which lead to disastrous consequences to urban area or infrastructure. In particular, because of advantages of low construction cost, the ability to screen large boulders, and increased hydraulic continuity, the use of rigid baffles (cylindrical or rectangular shape) and a flexible barrier with wire mesh among open-type debris flow countermeasure has been independently utilized recently. The baffles aim to decelerate frontal velocity and to reduce dynamic energy by impeding mobility of debris flow. The flexible barrier has an advantage in filtering debris materials and inducing deposition with absorbing dynamic energy of debris flows. If rigid baffles and a flexible barrier are installed sequentially in the flow path of debris flows, they can work as effective countermeasures against debris flows.

Figure 1 shows the concept of the multiple countermeasures, which combined with arrays of baffles and a flexible barrier. However, there has been no design guidelines for the configuration of baffles and they are still constructed based on empirical approaches by engineers. In particular, not only the appropriate specification and arrangement for baffle design has still not been suggested but also the energy reduction due to frictional loss among grains in design of flexible barrier has not been considered, which can accordingly lead to excessive design and increased cost. To understand the dynamic behavior of debris flows, dynamic interaction and energy dissipation caused by debris flow countermeasures, most of researchers have conducted debris flow experiments using artificial and miniaturized flumes [1, 5, 9, 12, 15]. The debris flow in small-scale flume, however, may exhibit disproportionalities in terms of viscous shear and pore pressures due to scale effect of flow [6]. Furthermore, because these flumes were straight and had a constant cross section, it was also difficult to investigate the topographic changes due to erosion and deposition during flow process.

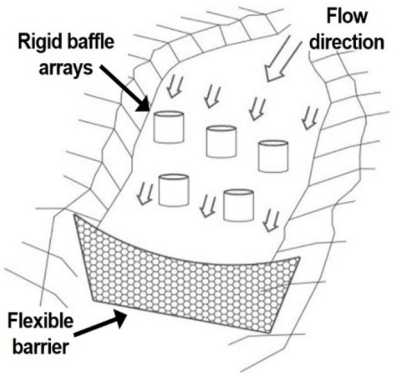

Fig. 1. The concept of multiple countermeasures

In this study, to investigate the flow characteristics by multiple countermeasures, real-scale experiment was conducted in a natural gully by reproducing a debris flow with a installation of multiple countermeasures. In

* Corresponding author: yune@gwnu.ac.kr

addition, topographic changes by the debris flow before and after experiment were investigated using UAV-LiDAR. Video cameras were installed along the flow path to capture the dynamic behavior of the debris flow. Load cells were installed in front of the baffles and the flexible barrier to measure the impact load. After the experiment, the frontal velocity and flow depth were estimated by the captured image profiles based on the video recordings. From the test data, the velocity reduction characteristics of the flow due to multiple countermeasure and the topographic changes due to the erosion and deposition of the gully by the debris flow were analyzed.

2 Real-scale debris flow experiment

2.1 Test site

Figure 2 shows the study area of the real-scale debris flow experiment, which is located at Jinbu, Gangwon province, South Korea. The watershed area of the study site is 0.28 km^2, with a main channel having an overall length of 824 m and minimum and maximum width of 4.6 and 13.7 m, respectively. The inclination of the initiation zone and downstream area of the main channel is 39° and 8°, respectively. It has a similar topographic characteristics with typical debris hazard sites in South Korea [14].

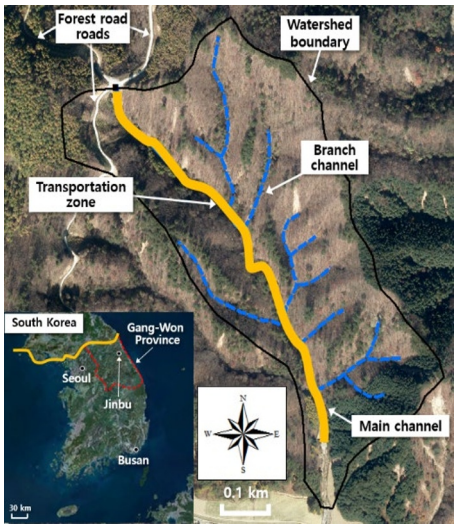

Fig. 2. Study area for the real-scale debris flow experiment.

2.2 Initiation facility and experimental conditions

Figure 3 shows schematic diagram of the debris flow initiation facility. The facility was 12.6 m in length and 12.0 m in width, consisted of a soil container at the front and a water container at the back. The height at the front and back of the facility were 6.5 m and 5.0 m, respectively. The maximum volume of soil and water container was 346 and 268 m^3, respectively. In this study, 262 m^3 of soil and 202 m^3 of water were used. Actual images of the debris flow initiation facility are shown in Figure. 4. Figure 5 shows the multiple countermeasures installed at the gully of downstream. The multiple countermeasures consist of rigid hollow cylindrical baffles with holes and a flexible barrier with wire mesh. The diameter and height for the cylindrical baffle was were 0.5 m and 2.0 m, respectively. Each spacing between successive rows and flexible barrier from baffle arrays was 12 m. The baffle arrays and flexible barrier were installed at 188 (first row of baffles) and 212 m, respectively, from the debris flow initiation facility. The transverse blockage ratio of baffles in the channel was determined as 40 % [7, 13]. The size of flexible barrier was 6.0 m (top) and 4.0 m (bottom) in width, and 3.0 m in height. The maximum allowable energy of the flexible barrier was 500 kJ. To measure dynamic impact load of debris flow, load cells were installed at the top, middle, and bottom of the front baffles. Shackle type-tension load cells were installed at the top, middle, and bottom on both sides of the flexible barrier as well. The detailed design and arrangement of multiple countermeasures for field experiment were determined based on the small-scale experiment [10].

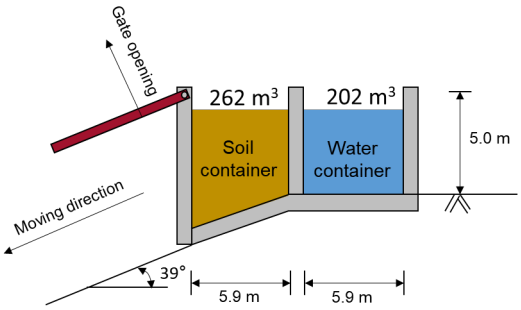

Fig. 3. Schematic diagram of debris flow initiation facility.

Fig. 4. Debris flow initiation facility at top view (left) and at front view (right).

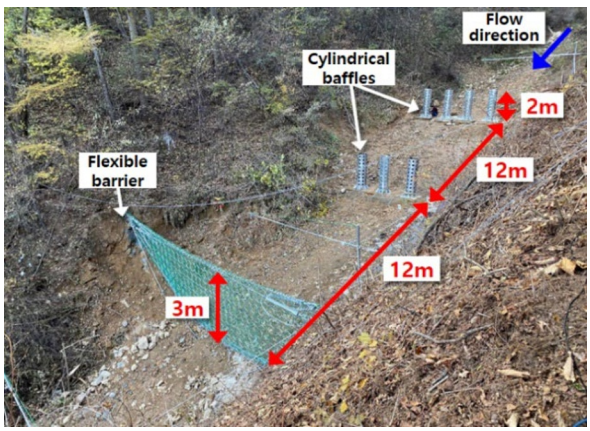

Fig. 5. Real-scale experiment setup.

2.3 UAV-LiDAR survey

To investigate the topographic changes in the channel due to the debris flow experiment, field surveys using UAV-LiDAR (DJI Matrice 600 pro; Velodyne VLP-16 puck) were performed before and after the experiment over the whole channel. The UAV was flown manually at an altitude from 60 m to 80 m above the ground with the velocity of approximately 0.5 m/s. By means of surveys performed two times, the point clouds before and after the real-scale debris flow experiment were obtained.

Removal of non-ground points is an essential step to calculate topographic changes. The non-ground points include trees and installed man-made structures such as cylindrical baffles, a closed-type barrier, a flexible barrier, and a debris storage container. These non-ground points were removed using the cloth simulation filtering (CSF) plug-in of CloudCompare [2, 16]. The cloth resolution of 1.0 m and the classification threshold of 2.0 m were used for the CSF. We chose the multiscale model to model cloud comparison (M3C2) method which is widely used among the point cloud comparison approaches to detect topographic height changes before and after the real-scale experiment [11]. In the M3C2 method, the projection scale D was set as 1.7 m. Note that the normal calculation was not implemented in this study as the orientation for comparison was pre-defined to be vertical. Figure 6 shows the digital elevation model (DEM) before and after vegetation filtering.

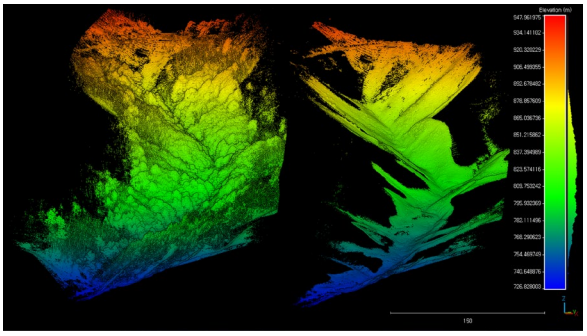

Fig. 6. Digital elevation model (DEM) before vegetation filtering (left) and after vegetation filtering (right).

3 Experiment results

3.1 Velocity of debris flow

Figure 7 shows the change of frontal velocity along the transportation zone. The altitude of debris flow initiation facility was 917m, and it gradually decreased along the channel as it went downstream. To figure out the effect of the multiple countermeasures on the frontal velocity of the debris flow, the results of the real-scale experiment conducted in 2012 without debris flow countermeasures was added in the figure [8]. In here, the square symbol (RT) and circle symbol (RT_M) indicate the case without and with the multiple countermeasures, respectively. The frontal velocity of debris flows for the two experiments showed a peak value right after the release of debris materials from the initiation facility due to a steep inclination in the initiation zone, and then slowed down until 140 m from the initiation facility. From 140 to 210 m, in case of the experiment without countermeasure, the frontal velocity increased because of the straight channel and exposed bed rock having a smooth surface. Thereafter, the slope became gentle around 8° in average, and accordingly the frontal velocity of debris flow gradually decreased. According to the recorded video of the experiment, the debris eventually stopped at 740 m away from the initiation zone.

By contrast, in the experiment with the countermeasures, the presence of the countermeasures significantly reduced the frontal velocity in the region between 188 m and 210 m away from the initiation zone. The frontal velocity was reduced by baffle arrays by 51% compared with the upstream flow before entering the baffles. Moreover, the frontal velocity further decreased as the debris flow passed through the flexible barrier. After the multiple countermeasures, the frontal velocity partly regained its speed again. Thus, the installation of the multiple countermeasures significantly decreased the dynamic energy of debris flows through suppression of flow mobility.

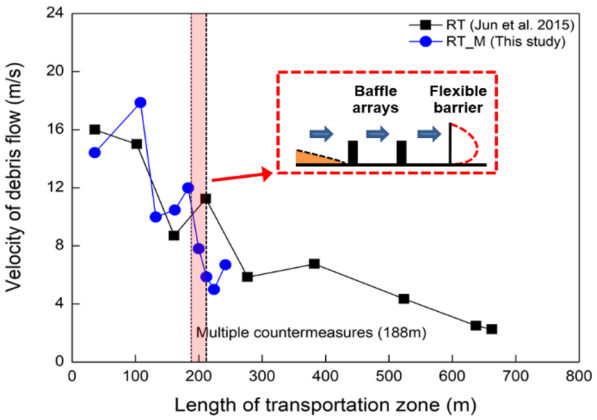

Fig. 7. Debris flow frontal velocity along transportation zone.

3.2 Topographic changes

Figure 8 shows the topographic map of the height alteration in the channel due to the debris flow, which was obtained by comparing LiDAR 3D point clouds using the M3C2 method. This two-dimensional topographic change map was generated through the rasterization of M3C2 distance profile with a cell size of 20 cm. Each cell represents elevation change; accordingly, the erosion and deposition volumes can be calculated at each cell. The total erosion volume was estimated as 2,872 m^3 and the deposition volume as 3,210 m^3, respectively. The result depicts the areas with active basal erosion and the trap and deposition of debris by the multiple countermeasures including the flexible barrier and baffles.

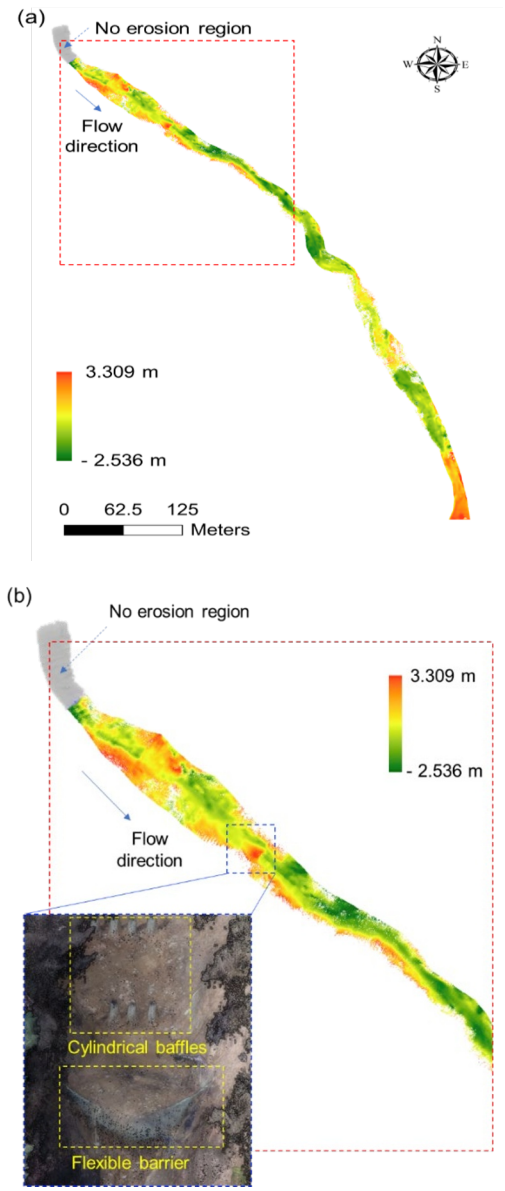

Fig. 8. Maps of topographic changes by debris flows: (a) the entire channel and (b) an enlarged map of the transportation zone with the countermeasures.

4 Conclusions

In this study, to examine the effect of multiple countermeasures on the flow characteristics of debris flow, we conducted a real-scale experiment in a natural gully with the installation of cylindrical baffles and a flexible barrier. The frontal velocity of the debris flow showed a significant increase and a maximum value in the upstream zone due to a high slope angle. But the installation of multiple countermeasures significantly reduced the frontal velocity at the downstream. The topographic changes by debris flow before and after the experiment were also investigated using UAV-LiDAR. The LiDAR results confirmed the effect of countermeasures which caused a large amount of results provide unique data on well-controlled real-scale debris flow tests, which can be readily extended for various parametric studies and used for numerical modelling development.

This research was supported by a grant (22RITD-C158631-03) from the Regional Innovation Technology Development Program funded by the Ministry of Land, Infrastructure and Transport of the Korean government. Support was also given by the Basic Science Research Program through the National Research Foundation of Korea (NRF) funded by the Ministry of Education (2021R1A6A1A03044326) and by "Ministry of the Interior and Safety" R&D program (20018265).

References

1. Chae. B.G, Song, Y.S, Seo. Y.S, Cho. Y.C, Kim. W.Y, J. E. Geol. **16**, 3 (2006), (In Korean)
2. CloudCompare, GPL Software, Version 2.10, (2019)
3. Hübl. J, Suda. J, Proske. D, Kaitna. R, Scheidl. C, *Debris flow impact estimation steep slopes*, in Proceedings of the 11th International Symposium on Water Management and Hydraulic Engineering, WMHE, 1–5 September 2009, Ohrid, Macedonia (2009)
4. Hungr. O, Morgan. G.C, Kellerhals. R, Can Geotech. J. **21**,4 (1984)
5. Iverson. R.M, Reid. M.E, Logan.M, LaHusen. R.G, Godt. J.W, Griswold. J.P, Nat. Geoscience **4** (2011)
6. Iverson, R.M, Denlinger. R.P, J Geophys. Res. Solid Earth **106** (2001)
7. Ikeya. H, Uehara. S, J. Jpn. Eros. Con. Eng. Soc. **114** (1980), (in Japanese)
8. Jun. K.J, Lee. S.D, Kim. G.H, Lee. S.W, Yune. C.Y, *Verification of countermeasures by velocity estimation of real scale debris flow test*, in Proceedings of the 6th International Conference on Debris flow Hazard Mitigation: Mechanics, Prediction and Assessment, DFHM6, 22–25 June 2015, Tsukuba, Japan (2015)
9. Kim. K, Lee. D, Kim. D, Lee. S, J. Kor. Geo. Environ. Mental. Soc. **9**, 5 (2008), (In Korean)
10. Kim. B.J, Kim. Dolla, Yune. C.Y, Korean Society of Hazard Mitigation, Conference, 9-10, September 2021 (in Korean), (2018)
11. Lague.D, Brodu.N, Leroux.J, Remote sensing J. P **82** (2013)
12. Scheidl. C, Chiari. M, Kaitna. R, Müllegger. M, Krawtschuk. A, Zimmermann, T, Proske. D, Surv. Geophys. **34**, 1 (2013)
13. Watanabe. M, Mizuyama T, Uehara.S, J. Jpn. Eros. Con. Eng. Soc. **115** (1980), (in Japanese)
14. Yune. C.Y, Kim. K.S, Yoo. N.J, Seo. H.S, Jun. K.J, Italian. J. E. Geol and Environ (2011)
15. Zhou. G.G.D, Li. S, Song. D, Choi, C.E, Chen. X, Landslides **16**, 2 (2018)
16. Zhang. W, Qi.J, Wan.P, Wang.H, Xie. D, Wang. X, Yan. G, Remote sensing, **8**, 6 (2016)